Marqués, MC.; Zamarbide-Forés, S.; Pedeleni, L.; Llopis Torregrosa, V.; Yenush, L. (2015). A functional Rim101 complex is required for proper accumulation of the Ena1 Na+-ATPase protein in response to salt stress in Saccharomyces cerevisiae. FEMS Yeast Research. 15(4):1-12. doi:10.1093/femsyr/fov017.

OXFORD UNIVERSITY PRESS | FEMS Yeast Research

http://mc.manuscriptcentral.com/fems

A functional Rim101 complex is required for proper accumulation of the Ena1 Na+-ATPase protein in response to salt stress in Saccharomyces cerevisiae

Journal:	*FEMS Yeast Research*
Manuscript ID:	Draft
Manuscript Type:	Research Article
Date Submitted by the Author:	n/a
Complete List of Authors:	Marqués, Mª Carmen; Instituto de Biología Molecular y Celular de Plantas (UPV-CSIC), Universitat Politécnica de Valencia-Consejo Superior de Investigaciones Científicas Zamarbide-Fores, Sara; Instituto de Biología Molecular y Celular de Plantas (UPV-CSIC), Universitat Politécnica de Valencia-Consejo Superior de Investigaciones Científicas Pedelini, Leda; Instituto de Biología Molecular y Celular de Plantas (UPV-CSIC), Universitat Politécnica de Valencia-Consejo Superior de Investigaciones Científicas Llopis-Torregrosa, Vicent; Instituto de Biología Molecular y Celular de Plantas (UPV-CSIC), Universitat Politécnica de Valencia-Consejo Superior de Investigaciones Científicas Yenush, Lynne; Institute of Plant Molecular and Cellular Biology, Lab 1.08
Keywords:	Ion transport, salt tolerance, ESCRT pathway

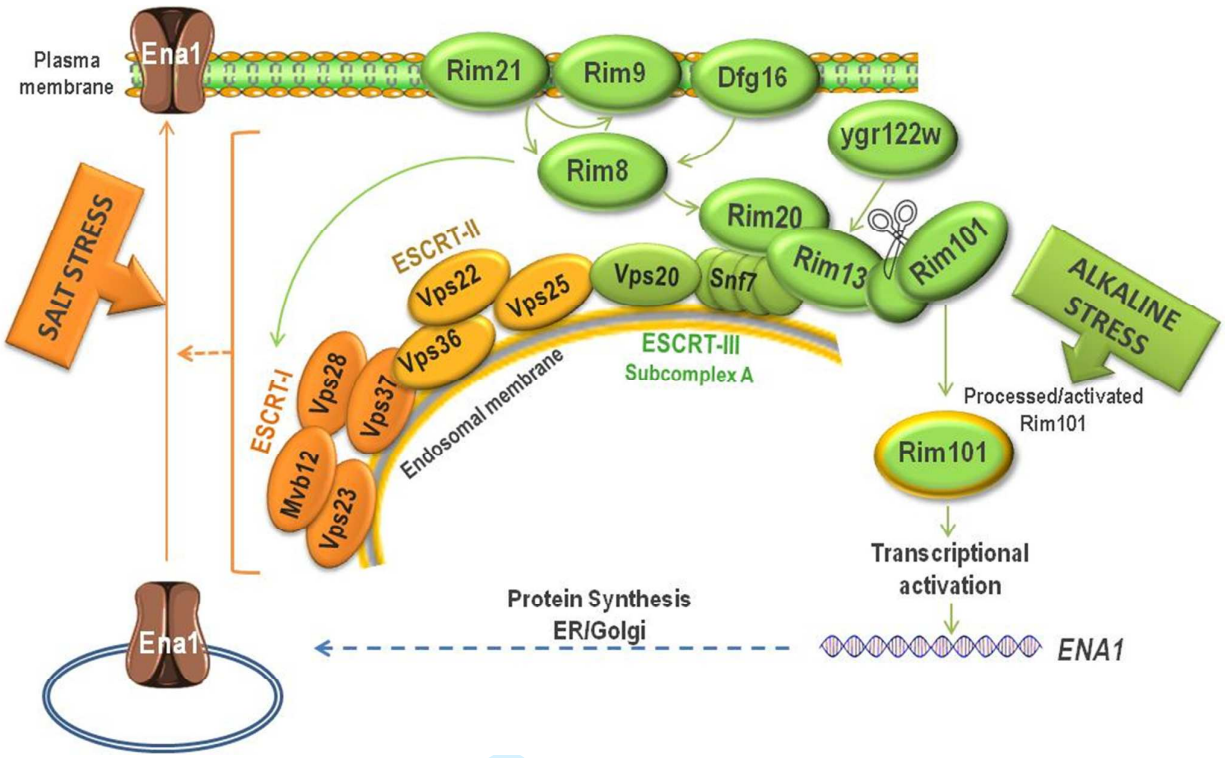
Plasma membrane
Ena1
Rim21
Rim9
Dfg16
ygr122w
Rim8
Rim20
Rim13
Rim101
SALT STRESS
ALKALINE STRESS
ESCRT-II
Vps22
Vps25
Vps20
Snf7
Vps36
ESCRT-III
Subcomplex A
ESCRT-I
Vps28
Vps37
Mvb12
Vps23
Endosomal membrane
Processed/activated Rim101
Rim101
Transcriptional activation
Protein Synthesis ER/Golgi
ENA1
Ena1

Title: A functional Rim101 complex is required for proper protein accumulation of the Ena1 Na^+-ATPase in response to salt stress in *Saccharomyces cerevisiae*

Authors: Mª Carmen Marques, Sara Zamarbide-Forés, Leda Pedelini, Vicent Llopis-Torregrosa[1], Lynne Yenush[#]

Affiliation: Instituto de Biología Molecular y Celular de Plantas (IBMCP), Universitat Politècnica de València-Consejo Superior de Investigaciones Científicas, Avd. de los Naranjos s/n, Valencia, Spain 46022

#Corresponding Author: Lynne Yenush
email: lynne@ibmcp.upv.es
phone: +34963879375
fax: +34963877859

Running title: Rim101 pathway required for proper Ena1 protein accumulation

Key words:
Ion transport
Rim101 pathway
ESCRT pathway

[1] Current address:
Vicent Llopis Torregrosa
Dpt. of Membrane Transport
Institute of Physiology ASCR, v.v.i.
Videnska 1083
CZ-14220 Prague 4
Czech Republic

Abstract:

The maintenance of ionic homeostasis is essential for cell viability, thus the activity of plasma membrane ion transporters must be tightly controlled. Previous studies in *Saccharomyces cerevisiae* revealed that the proper trafficking of several nutrient permeases requires the HECT family E3 ubiquitin ligase Rsp5 and, in many cases, the presence of specific adaptor proteins needed for Rsp5 substrate recognition. Among these adaptor proteins are the 9 proteins of the ART (Arrestin-Related Trafficking Adapter) family. We studied the possible role of the ART family in the regulation of monovalent cation transporters. We show here that the salt sensitivity phenotype of the *rim8*/*art9* mutant is due to severe defects in Ena1 protein accumulation, which is not attributable to transcriptional defects. Many components of the Rim pathway are required for correct Ena1 accumulation, but not for other nutrient permeases. Moreover, we observe that strains lacking components of the ESCRT pathway previously described to play a role in Rim complex formation present similar defects in Ena1 accumulation. Our results show that, in response to salt stress, a functional Rim complex via specific ESCRT interactions is required for the proper accumulation of the Ena1 protein, but not induction of the *ENA1* gene.

Introduction:

The dynamic regulation of the transport proteins present at the cell surface is vital for the successful adaptation of cells to their changing environment. Universally conserved mechanisms of ubiquitylation-dependent signal transduction routes are used to modify the cohort of receptors and transport proteins present under any given circumstances (MacGurn *et al.*, 2012). In both yeast and mammalians, the Nedd4-2 family of HECT domain E3 ubiquitin ligases have been shown to be important in this regulatory process (Yang & Kumar, 2010). In yeast, the sole Nedd4-2 homologue, Rsp5, regulates the trafficking of a large number target proteins by specifically catalyzing their ubiquitylation (Lauwers *et al.*, 2010).

Rsp5, like other Nedd4-2 family proteins, contains a C2 domain, required for plasma membrane association, in its N-terminus and a C-terminal HECT E3 ubiquitin ligase domain which flank three central WW domains (Wang *et al.*, 1999). These WW domains mediate protein-protein interactions by binding to so-called PY motifs. In yeast, it is known that the majority of the Rsp5 substrates do not contain PY motifs and therefore require the presence of Rsp5 adaptor proteins for their recognition. At least 19 different adapter proteins, including Bul1, Bul2 and members of the more recently denominated Arrestin-related trafficking (ART) protein family have been shown to function as Rsp5 adaptors (Leon & Haguenauer-Tsapis, 2009). This hierarchical organization provides a versatile system that can be regulated to orchestrate the dynamic post-translational regulation of plasma membrane transport proteins in response to environmental changes.

The majority of the known Rsp5 cargo proteins are nutrient permeases and divalent cation transporters (Lauwers *et al.*, 2010). However, knowledge is still lacking regarding the possible role for Rsp5-dependent signaling in the regulation of monovalent cation transporters. Monovalent cation homeostasis is crucial for the maintenance of several important physiological parameters, such as internal pH, turgor pressure and membrane potential. In mammals, Nedd4-2 is known to regulate the endocytosis of cation transporters, such as the ENaC sodium channel and CFTR Cl^- channel (Rotin & Staub, 2011). Therefore, it stands to reason that Rsp5 may also be involved in the regulation of yeast monovalent cation transporters.

In *Saccharomyces cerevisiae*, the transporters governing ion homeostasis have been well-characterized. The major plasma membrane transport proteins involved in this process include the plasma membrane H^+-ATPase, Pma1, the H^+/Na^+ antiporter, Nha1, the high affinity K^+-uptake system encoded by the *TRK1* and *TRK2* genes, and the Na^+ ATPase, Ena1 (Arino *et al.*, 2010). The regulation of the trafficking of these proteins has not been extensively studied. Although there are no reports regarding Nha1 trafficking, in the case of Pma1, many studies have addressed the trafficking of misfolded mutant isoforms and have shown that Pma1 is present in specialized sphingolipid-enriched microdomains in the plasma membrane (Bagnat *et al.*, 2001, Liu & Chang, 2006). We reported that the stability of the Trk1 K^+ transporter at the plasma membrane is compromised in mutants lacking the *SAT4/HAL4* and *HAL5* genes encoding related protein kinases (Perez-Valle *et al.*, 2007). In the absence of Hal4 and Hal5, Trk1, and several nutrient permeases, such as Can1 and Mup1, known to be regulated by the ART-Rsp5 pathway, are aberrantly delivered to the vacuole. However, the molecular mechanism by which the Hal4 and Hal5 kinases intervene in transporter trafficking is still unknown.

The regulation of the Ena1 Na^+-ATPase has been extensively studied, especially at the level of transcription. This gene is expressed at low levels under normal growth conditions, but its expression is markedly up-regulated in response to several stresses by multiple signaling pathways, including the Hog1 MAP kinase, the TOR pathway, the glucose repression pathway, the calcineurin pathway and the Rim101 pathway (Ruiz & Arino, 2007). Under mild salt or osmotic stress, the Hog1 and calcineurin pathways are principally responsible for *ENA1* induction through the regulation of the Sko1 repressor and the Crz1 activator respectively, although the TOR and glucose repression pathways also contribute to this regulation (Marquez & Serrano, 1996, Alepuz *et al.*, 1997, Proft & Serrano, 1999, Crespo *et al.*, 2001). In response to alkaline stress, *ENA1* induction is dependent on the Rim101, calcineurin and Snf1 pathways, (Lamb *et al.*, 2001, Serrano *et al.*, 2002, Lamb & Mitchell, 2003, Platara *et al.*, 2006). In terms of Ena1 trafficking, Adler and colleagues have shown that the Sro7 protein is involved in correct delivery of Ena1 to the plasma membrane (Wadskog *et al.*, 2006). In mutants lacking *SRO7*, the Ena1 protein is routed to the vacuole for degradation. Another study, reported by Logg

and collaborators, showed that Ena1 localization to the plasma membrane was severely delayed in several vps mutants that display salt sensitivity (Logg *et al.*, 2008). Interestingly, some of these vps mutants analyzed in this study were ESCRT components. The ESCRT complex is known to be involved in the sorting of plasma membrane transport proteins ubiquitylated by Rsp5 to multivesicular bodies for subsequent degradation in the vacuole (MacGurn *et al.*, 2012).

As two independent lines of evidence suggest a possible link between Rsp5-mediated regulation and monovalent cation transport proteins, we systematically analyzed the role of Rsp5 adaptor proteins in salt tolerance. We uncover a novel role for the Rim101 pathway in the proper plasma membrane accumulation of the Ena1 Na^+-ATPase.

Materials and Methods:

Yeast strains and culture conditions. All strains of *S. cerevisiae* used in this work are derived from the BY4741 background. All single mutant strains were obtained from the EUROSCARF collection (BY4741). The *ena1-5* mutant strain was kindly provided by Dr. Hana Sychrová (Zahrádka & Sychrová, 2012). The *hal4 hal5* strain has been described previously (Perez-Valle *et al.*, 2010). YPD contained 2% glucose, 2% peptone, and 1% yeast extract. In the case of the alkaline YPD media, the pH was adjusted to 8.0 using TAPS ([(2-Hydroxy-1,1-bis(hydroxymethyl)ethyl)amino]-1-propanesulfonicacid). Minimal medium (SD) contained 2% glucose, 0.7% yeast nitrogen base (Difco) without amino acids, 50 mM succinic acid adjusted to pH 5.5 with Tris, and the nutritional components required by the strains. Growth assays were performed on solid media by spotting serial dilutions of saturated cultures onto plates with the indicated composition. Images were taken after 2-4 days of growth.

Plasmids and genomic integrations. The pCM262-*ENA1*-GFP plasmid was constructed by homologous recombination in yeast using the pCM262 plasmid containing the GFP coding sequence inserted into the PstI site. This vector is derived from pCM190 and it contains tetracycline-responsive promoter (Garí *et al.*, 1997). The *ENA1* coding sequence was amplified by PCR from genomic DNA using the following primers: Ena1-recomb-5'-tac cgg atc aat tcg ggg gat cag ttt ATG GGC GAA GGA ACT ACT AA; Ena1-recomb-3'-cat aag ctt ctg cag gcg gcc gcg ttt TTG TTT AAT ACC AAT ATT AAC TTC. The plasmid was linearized using *Pme*1, dephosphorylated and co-transformed into the *ena1-4* mutant with the *ENA1* PCR fragment. Positive clones were selected first by growth in media without uracil (+DOX) and then by growth in media containing 0.1M LiCl (-DOX). Plasmids were recovered from candidate clones, transformed into *E. coli*, purified and confirmed by sequencing. The plasmid used for the β-galactosidase assays YEp-*ENA1*prom-lacZ was described previously (Marquez & Serrano, 1996). The coding sequence for GFP was integrated at the 3' of the *ENA1* gene by homologous recombination using a cassette amplified from the pFA6a-GFP(S65T)-HIS3MX6 plasmid (Longtine *et al.*, 1998) containing the *HIS3* selection gene using the following primers: *ENA1* F2: 5'-TACTACAATCCATACAGAAGTTAATATTGGTATTAAACAA CGG ATC CCC GGG TTA ATT AA-3'; *ENA1* R1: 5'-TGAATAAGGAAAAAGATAGGGAGCACTTAATAGGCCCTGC GAATTCGAGCTCGTTTAAAC-3'. The correct insertion of the integration cassette was confirmed by genomic PCR using the following primers: forward primer- (anneals at base pair 3205 of *ENA1*) and reverse primer-5'-TTTGTATAGTTCA TCCATGCC-3' (anneals at the 3' end of the GFP gene). The *RIM101-155* plasmid was kindly provided by Aaron Mitchell (Subramanian *et al.*, 2012).

Protein extraction and fractionation. Protein extracts, fractionation procedures and immunoblot analyses were performed as described (Perez-Valle *et al.*, 2007).

Confocal microscopy. Fluorescence images were obtained for exponential phase live cells using the Zeiss 780 confocal microscope with excitation at 488 nm and detection at 510-550 nm for GFP (objective: plan-apochromat 40X/1.3 OIL DIC M27, ZEN 2012 software).

ß-Galactosidase assays. Yeast cells transformed with the indicated reporter plasmid containing the lacZ gene under the control of the *ENA1* promoter were grown selectively in SD medium and then diluted in YPD. Cells were grown to exponential phase, treated for the indicated time

with 0.5 M NaCl and then harvested by centrifugation (3000 rpm for 5 minutes). ß-Galactosidase activity was determined as described elsewhere and represented as ß-galactosidase activity units (Gaxiola *et al.*, 1992).

Northern Blot Analysis. Total RNA was isolated from yeast cells that were grown to mid log-phase in YPD. Cells were treated with 0.5 M NaCl and collected by centrifugation at the indicated times. Approximately 20 μg of RNA per lane was separated in formaldehyde gels and transferred onto nylon membranes (Hybond-N; Amersham). Radioactively labeled probes were hybridized in PSE buffer (300 mM sodium phosphate [pH 7.2], 7% sodium dodecyl sulfate, 1 mM EDTA). Probes used were as follows: a 0.5 kb PCR fragment representing nucleotides 1-500 of the *ENA1* gene and nucleotides 77-706 of *TBP1*, amplified from chromosomal yeast DNA. Signal quantification was done using a Fujifilm BAS-1500 phosphorimager.

Real-time luciferase assays. The dynamics of *ENA1* gene expression was measured using the pAG413-lucCP$^+$ plasmid containing 993 bp of the *ENA1* promoter (bp -1000 to -7, relative to the ATG) inserted upstream of the destabilized firefly luciferase gene. The indicated sequence of the *ENA1* promoter was amplified using the following primers: ENA1-PROM-pAG413luc F 5'- GTGACAGAGCTCGTCAATATTTTAGGGTTATCGGTG-3' and ENA1-PROM-pAG413luc R 5'-ATTCAGCAGCTGTTTCAATTCTGTGTACGAAG-3', which contain *Sac*I and *Pvu*I recognition sites, respectively. The digested PCR product was ligated into the *Sac*I/*Sma*I sites of the pAG413-lucCP$^+$ vector. The resulting plasmid, pAG413-*ENA1*-lucCP$^+$ was confirmed by sequencing and transformed into the indicated strains. Assays were performed as described (Rienzo *et al.*, 2012).

Sodium measurements. Sodium was measured by atomic absorbance spectrometry as described (Mulet *et al.*, 1999). Briefly, cells were grown in YPD to a final absorbance of 0.8-1.0. For measuring Na^+ uptake, cells were centrifuged, resuspended in YPD containing 0.5 M NaCl and incubated at 28ºC. Aliquots of 5 mL were taken at several time points, centrifuged for 5 minutes at 2000 *g* and washed twice with ice-cold washing solution (20 mM $MgCl_2$ and 180 mM sorbitol). The cell pellets were resuspended in 0.8 mL of cold washing solution, centrifuged again, and resuspended in 0.5 mL of 20 mM $MgCl_2$. Ions were extracted by heating the cells for 15 minutes at 95ºC. After centrifugation, aliquots of the supernatant were analyzed with an atomic absorption spectrometer (Varian) in flame emission mode. For sodium efflux experiments, the cells were incubated for 3 hours with the indicated concentration of NaCl as described above, centrifuged, washed once, and resuspended in YPD without salt. Aliquots of 5 mL were processed as indicated above.

Results:

Salt tolerance phenotypes of Rsp5 adapter mutants

As mentioned above, many previous studies have established a role for the Rsp5 ubiquitin ligase as an important regulator of plasma membrane proteins (Horak, 2003). These studies have also identified a set of proteins, known as Rsp5 adaptor proteins, which are required for correct cargo recognition (Leon & Haguenauer-Tsapis, 2009). We sought to examine if these proteins, and thus possibly Rsp5-mediated regulation, play a role in monovalent cation transporter regulation. As a first approach, we analyzed the salt sensitivity of strains lacking the genes encoding 15 different Rsp5 adaptor proteins, using the salt tolerant *ppz1* mutant and the salt sensitive *hal4 hal5* mutants for comparison. Here, we report the results obtained for strains lacking 9 genes encoding proteins classified as ARTs, as no notable phenotypes were observed for the other Rsp5 adapter mutants tested (*bul1*, *bul2*, *bsd2*, *ear1*, *ssh4*, and *tre1*, data not shown). As shown in Figure 1, we observe a slight, but reproducible tolerance to LiCl in strains lacking *LDB19* (also known as *ART1*). However, the most notable phenotype is the salt sensitivity of the *rim8* (*art9*) mutant. This observation is in agreement with previously published reports (Giaever *et al.*, 2002, Yoshikawa *et al.*, 2009, Herrador *et al.*, 2010, Zhao *et al.*, 2010).

Analysis of ENA1 gene expression and protein function in rim8 and rim101 mutants

Rim8 (Art9) is a component of the Rim101 alkaline response pathway, which is known to regulate the gene expression of the Ena1 P_2-type ATPase responsible for K^+, Na^+ and Li^+ extrusion (Treton *et al.*, 2000, Lamb *et al.*, 2001). Therefore, we tested *ENA1* expression in both *rim8* and *rim101* mutants grown under mild salt stress using real-time luciferase activity driven from the *ENA1* promoter, northern analysis, and β-galactosidase assays using the full *ENA1* promoter fused to the lacZ reporter gene. As shown in Figures 2A-C, in contrast to what has been observed for alkaline stress, we observed only a modest reduction in *ENA1* expression under these conditions (Lamb *et al.*, 2001, Serrano *et al.*, 2002, Platara *et al.*, 2006). This result is in agreement with a previous report and is likely explained by the dominant role played by the Hog1 MAP

kinase in the induction of *ENA1* under these conditions (Marquez & Serrano, 1996, Platara *et al.*, 2006).

We next monitored the accumulation of the Ena1 protein under these same conditions in wild type, *rim8* and *rim101* mutants containing GFP integrated at the 3' of the *ENA1* coding sequence. As Ena1-GFP was undetectable in the *rim8* and *rim101* mutants in crude extracts, we analyzed the insoluble fraction which contains membrane imbedded proteins, such as Pma1 and Trk1 (Perez-Valle, 2007). As shown in Figure 3A, we observe a drastic decrease in the amount of full-length Ena1 in both *rim8* and *rim101* mutants. We included the *crz1* mutant strain as a control. As expected, less Ena1 protein accumulates in response to salt stress in the *crz1* mutant as compared to the wild type control, but Ena1 accumulates to much higher levels than those observed in the *rim8* and *rim101* mutants (note exposure times in figure legend).

These results suggest that both the *rim8* and *rim101* mutants present defects in Ena1 protein accumulation, which should correspond to a decrease in Ena1 function. Accordingly, we examined the sodium loading and extrusion in these strains to determine if the observed decrease in Ena1 protein levels in the *rim8* and *rim101* mutants was functionally relevant. We observed no differences in the initial rate of sodium loading, suggesting that the membrane potential is not affected in any of the mutants tested. This result indicates that the function of the major determinants of plasma membrane potential, Pma1 and Trk1, are likely intact in these mutants. At longer time points we observed a three-fold increase in sodium loading in the *rim8* and *rim101* mutants (Figure 3B). These results suggest that the decrease in sodium loading observed in the wild type strain, which is principally due to the accumulation of the Ena1 protein at the cell surface, is impaired in the *rim8* and *rim101* mutants. This result is in good agreement with the observations described above and demonstrates that the *rim8* and *rim101* mutants present a clear defect in Ena1 function. Moreover, we also observe a decreased extrusion rate in both Rim pathway mutants, relative to the wild type control (Figure 3C). As expected, these phenotypes were less severe than that observed for the complete *ena1-5* mutant, but indicate a notable decrease in Ena1 function in the *rim8* and *rim101* mutants, which leads to a three-fold increase in sodium accumulation. Since these experiments are carried out in YPD media (pH 6.5),

Ena1 activity dominates over that of the Nha1 Na^+/H^+ antiporter, which is active under acidic growth conditions (Bañuelos *et al.*, 1998). Given the mild effect on the *ENA1* gene expression profile and the marked effect on Ena1 protein accumulation, we propose that the reduction in Ena1 protein accumulation and function shown here may correspond to post-transcriptional defects.

In order to determine whether the Ena1 accumulation defect observed in the *rim8* mutant are attributable to Rim101-dependent transcriptional effects, we transformed strains with a plasmid harbouring a constitutively active form of Rim101: *RIM101-511* (Subramanian *et al.*, 2012). We tested the *rim8* mutant and control strains containing the *ENA1*-GFP genomic fusion for both salt sensitivity and Ena1 plasma membrane accumulation. As observed in Figures 4A and 4B, the constitutively active Rim101 allele, which confers salt tolerance in the wild type strain, only partially rescues the salt sensitivity of the *rim8* mutant and only slightly improves Ena1 accumulation. Some rescue of the salt sensitivity phenotype is expected, since overexpression of the constitutively active form of *RIM101* will clearly cause an increase in *ENA1* expression irrespective of the environmental conditions. However, the fact that this increase in *ENA1* expression does not recover the *rim8* phenotype in conditions of salt stress indicates that the decrease in Ena1 accumulation in the *rim8* mutant is not due only to improper processing of the Rim101 transcription factor and is consistent with the hypothesis that Ena1 does not accumulate properly in the plasma membrane in this mutant.

In order to confirm this observation and to facilitate detection of Ena1-GFP in the *rim8* or *rim101* mutants by fluorescence microscopy (the very low levels of the integrated Ena1-GFP were undetectable), we constructed a plasmid containing the *ENA1*-GFP sequence under control of an inducible promoter. As shown in Figure 5A, overexpression of Ena1 only partially rescues the salt sensitivity phenotype of these mutants, even though the promoter is no longer controlled by the Rim101 pathway. This result confirms the observations made using the *RIM101-511* allele. Upon analysis of the Ena1-GFP protein profile in immunoblots, in addition to the Ena1-GFP band, we observed a marked accumulation in lower molecular weight bands, likely corresponding to Ena1-GFP degradation products in the *rim8* and *rim101* mutants

(Figure 5B). When we examined the fluorescence pattern in these strains, we observed mislocalization of Ena1-GFP in both mutants (Figure 5C). Although detectable amounts of overexpressed Ena1-GFP appear to arrive to the plasma membrane, explaining the partial phenotypic rescue, we also observe aberrant signal in the interior of the cell. This signal inside the cell indicates that Ena1 is not efficiently targeted to the plasma membrane, but accumulates internally. Interestingly, this phenotype is qualitatively different than that observed in *sro7* mutants. In the case of *sro7* mutants, the Ena1 signal accumulates in the vacuole, not in the cell interior (Wadskog *et al.*, 2006). Our results clearly show that Ena1-GFP does not accumulate in the vacuole in *rim8* and *rim101* mutants.

Importantly, these results demonstrate that the *rim8* and *rim101* mutants are unable to efficiently deliver and/or maintain the Ena1-GFP protein at the cell surface under conditions of salt stress. These results are in stark contrast with the currently proposed model for salt sensitivity of the Rim pathway mutants, which contends that the defect resides in defective *ENA1* transcription. We propose that under physiological expression levels, such as those observed in Figure 2, the observed defects in Ena1 accumulation contribute to the salt sensitivity of the *rim8* and *rim101* mutants.

In order to determine if the Ena1-GFP plasma membrane accumulation defect in *rim8* and *rim101* mutants is due to a general defect in transporter trafficking, we tested the steady-state accumulation of the tryptophan permease, Tat2, and the methionine starvation-induced delivery of the Mup1 permease to the plasma membrane. As observed in Figure 6, no defect was observed in either case, suggesting that not all plasma membrane proteins are affected in *rim8* and *rim101* mutants. We also confirmed the proper delivery of Mup1 to the plasma membrane by confocal microscopy (data not shown).

Salt tolerance and Ena1 accumulation in Rim101 pathway and ESCRT mutants

We then tested whether other components of the Rim101 pathway have similar Ena1 accumulation defects. For this, we analyzed both the salt sensitivity of Rim101 pathway mutants and the protein pattern of Ena1-GFP expressed ectopically under the control of an inducible promoter, as described above (Figures 7A and B). Mutants

lacking genes encoding all components of the Rim101 protein complex showed similar phenotypes in both salt sensitivity and aberrant Ena1-GFP accumulation, again indicating a defect in the accumulation of the Ena1 protein. Ena1 accumulated normally in strains lacking the genes encoding the Rim15 kinase and the Nrg1 transcriptional repressor, as expected. The Rim15 kinase was identified in the original screen looking for mutants with reduced ability to undergo meiosis, but was subsequently shown to be a glucose-repressible regulator of Ime1-Ume6 complex formation required to activate the expression of many meiotic or sporulation-specific genes (Vidan & Mitchell, 1997). The Nrg1 protein has been shown to act as a negative regulator of *ENA1* expression and so its effect is predicted to be purely transcriptional (Lamb *et al.*, 2001). As expected, neither of these mutants presents salt sensitivity phenotypes. This data suggest that that disruption of the functional Rim101 signaling complex negatively affects the proper accumulation of Ena1 at the plasma membrane. Therefore, the formation of this multi-protein complex has an important impact on Ena1 protein accumulation, in addition to its well-known role in Rim101 transcription factor processing.

Work from several laboratories studying the Rim101 pathway in both *S. cerevisiae* and *A. nidulans* has shown a physical and functional interaction with components of the ESCRT vesicular trafficking pathway (reviewed in (Maeda, 2012)). Moreover, it has recently been shown that this complex forms at the plasma membrane (Galindo *et al.*, 2012, Obara & Kihara, 2014). More specifically, it has been shown that the components of the ESCRT-I, ESCRT-II, and the Snf7 and Vps20 ESCRT-III components form a physical complex with Rim components and are required for proper Rim101 processing and therefore its transcriptional activity (Xu *et al.*, 2004, Hayashi *et al.*, 2005, Calcagno-Pizarelli *et al.*, 2011). As our data suggest defect in Ena1 accumulation at the plasma membrane in Rim pathway mutants, we tested whether the all the components of the ESCRT pathway previously described to interact with the Rim101 signaling complex also display salt sensitivity and Ena1 protein accumulation defects. As shown in Figure 8, we observed an excellent correlation between components of the ESCRT machinery previously described to interact with the Rim complex and salt sensitivity (Figure 8A). These same mutants also displayed notable decreases in Ena1-

GFP accumulation, consistent with previous results analyzing some of these same vps mutants (Logg *et al.*, 2008). In fact, the effect appears even more severe for these mutants, than for the Rim pathway mutants, as may be expected since vps mutants are known to have general effects on several aspects of vesicle trafficking. Importantly, as reported by Logg and colleagues, we observed internal accumulation of Ena1-GFP, similar to that observed in the *rim8* and *rim101* mutants, in several of the *vps* mutants studied (data not shown and (Logg *et al.*, 2008)). Interestingly, mutant strains lacking the two ESCRT-III components, *VPS24* and *DID4*, required for MVB sorting of ubiquitylated cargo proteins, but not for the formation of a functional Rim101 complex do not display salt sensitivity or Ena1 accumulation defects. These data suggest that the proper formation of the complete Rim/ESCRT complex, rather than the MVB-related ESCRT function, is required for efficient Ena1 plasma membrane accumulation. This hypothesis is further supported by the lack of phenotypes presented by the ESCRT-0 component mutant *vps27*. As the Ena1 accumulation experiments are performed using a heterologous promoter for *ENA1* expression that does not respond to the Rim101 transcription factor, our data suggest an additional role for the Rim/ESCRT complex in Ena1 protein accumulation, which is independent of the transcriptional activation of the *ENA1* gene.

Discussion:

It is well known in mammals that the endocytic regulation of various monovalent cation transporters plays an important role in many aspects of ion homeostasis (reviewed in (Mulet *et al.*, 2013)). Perhaps the best-studied example is the Nedd4.2-dependent regulation of the ENaC sodium transporter. Several biochemical and genetic studies in both mouse and humans have shown that alterations in the ubiquitylation of ENaC cause the aberrant accumulation or reduction in the levels of this sodium transporter, leading to Liddle's Syndrome and hyperkalaemic acidosis, pseudohypoaldosteronism type 1, respectively (Chang *et al.*, 1996, Schild *et al.*, 1996, Staub *et al.*, 1996, Abriel *et al.*, 1999). In yeast, a role for the Nedd4.2 orthologue, Rsp5 in regulating monovalent cation homeostasis is only beginning to be considered. We have taken a systematic approach to determine the relevant phenotypes of mutants lacking genes encoding Rsp5 adaptor proteins to address this question. Here, we present data on the phenotypic characterization of 9 ART family member mutants.

The most significant phenotype observed in this analysis is the LiCl and NaCl sensitivity of the mutant lacking the gene encoding *RIM8* (also known as *ART9*). This α-arrestin-related protein is known to play a key role in the regulation of the alkaline stress response pathway named for the Rim101 transcription factor (Treton *et al.*, 2000, Herranz *et al.*, 2005, Herrador *et al.*, 2010). The *rim101* mutant was previously reported to be sensitive to both alkaline pH and salt stress (Lamb *et al.*, 2001, Lamb & Mitchell, 2003). As the P-type Na^+ ATPase encoded by the *ENA1* gene is a known target of the Rim101 transcription factor in response to alkaline stress, the salt sensitivity phenotype was also attributed to a defect in *ENA1* induction (Lamb & Mitchell, 2003). This idea is supported by the phenotypic rescue observed upon further deletion of the Ngr1 repressor in the *rim101* background. However, detailed analysis of *ENA1* induction in response to salt stress in the *rim101* mutant has not been reported. Here, we examined *ENA1* induction by real-time luciferase, northern, and β-galactosidase assays in both the *rim101* and *rim8* mutants. We observe only a modest reduction in the salt responsiveness of the *ENA1* gene when compared to the isogenic wild type control strain, likely due to the dominant role played by the Hog1 pathway under these conditions (Figure 2) (Platara *et al.*, 2006).

In parallel, we examined the amount of Ena1 protein in the same mutants by immunoblot using strains in which the open reading frame of GFP was inserted into the genome downstream of the *ENA1* gene. Using this approach, we observed a striking reduction in the amount of full-length Ena1 in both the *rim8* and *rim101* mutants (Figure 2). This reduction is unlikely to be explained by the modest decrease in *ENA1* transcription observed under the same experimental conditions, and indeed *rim8* strains expressing a constitutively active version of Rim101 still had important defects in Ena1 accumulation. We confirmed the decrease in Ena1 function by performing sodium loading and extrusion assays. We observe that both the *rim8* and *rim101* mutants accumulate three fold more sodium as compared to the wild type strain after two hours and also display a significant reduction in the initial rate of sodium extrusion (Figure 3). Importantly, we also observe a defect in Ena1-GFP localization in both mutant strains, supporting a role for the Rim101 pathway in proper Ena1 protein accumulation at the plasma membrane (Figure 4). Although a portion of overexpressed Ena1 arrives to the cell surface, consistent with the partial phenotypic rescue, the protein also accumulates internally (non-vacuolar), in a pattern reminiscent of that reported by Logg and collaborators for the class E vps mutants they tested: *vps4*, *vps20*, *snf7* and *snf8* (Logg *et al.*, 2008). This defect could reflect alterations in the delivery of Ena1 from the ER/Golgi to the plasma membrane or recycling of endocytosed vesicles back to the plasma membrane. Further experiments will focus on characterizing this phenotype.

We propose that this defect in Ena1 protein accumulation of will be more relevant under endogenous expression levels and is likely to explain the salt sensitivity and sodium loading and extrusion defects observed in these mutants. Importantly, this defect in Ena1 plasma membrane delivery and/or accumulation expressed from a plasmid under the control of an exogenous promoter is clearly independent of the Rim101-dependent regulation of the *ENA1* promoter and supports a role for this pathway in the post-translational regulation of this transporter. The fact that a constitutively active form of Rim101 only partially rescues the salt sensitivity and Ena1 accumulation defect of the *rim8* mutant lends further support to this hypothesis. However, it is also possible that other Rim101-responsive genes are implicated in

proper Ena1 accumulation. In any case, our data clearly indicate that, under the conditions tested, defective *ENA1* induction is not observed and therefore does not explain the salt sensitivity of the *rim101* and *rim8* mutants. We propose that the defect is related to the inability to accumulate sufficient amounts of functional Ena1 at the plasma membrane.

Several lines of evidence have connected the function of the Rim101 pathway with the subclass of *vps* mutants that belong to the ESCRT machinery (reviewed in (Maeda, 2012)). For example, physical interactions have been reported between Rim8 and both Stp22 and Vps28 (ESCRT-I components) and between Snf7 (ESCRT-III component) and Rim20 and Rim13 (Ito *et al.*, 2001, Xu & Mitchell, 2001, Xu *et al.*, 2004, Herrador *et al.*, 2010). Moreover, Rim20 was found to co-localize with Snf7 in vesicles that accumulate under alkaline stress in *vps4* mutants (Boysen & Mitchell, 2006). A role for the ESCRT pathway in Rim101 activation has also been reported. Xu and collaborators showed that the same subset of ESCRT mutants studied here present defects in Rim101 processing (Xu *et al.*, 2004). These mutants are thought to be defective in the formation of a functional Rim101 complex. In this study they also showed that the Rim101 processing defective mutants are sensitive to LiCl. In agreement with these results, we have shown here that these mutants are also NaCl sensitive and accumulate much lower levels of Ena1 at the plasma membrane, even when expressed from an exogenous promoter. This point is important, as it shows that the decrease in Ena1 protein accumulation observed in these mutants is not due to a decrease in Rim101-dependent transcription, since the promoter used does not respond to this pathway. Taken together, these results support a model in which Ena1 protein accumulation is influenced by the ESCRT/Rim101 complex independently of Rim101-dependent transcriptional activation of the *ENA1* gene under conditions of salt stress.

These data provide evidence for a novel function of the Rim101 complex in Ena1 protein accumulation, in addition to its well-established role in transcriptional regulation. It is conceivable that alterations in the Rim101-dependent transcription of genes other than *ENA1* are involved in the observed defect in Ena1 protein trafficking, but the mild rescue of the *rim8* phenotypes using the constitutively active *RIM101-511* allele or expressing *ENA1* from an exogenous promoter argues against this possibility.

Future experiments will determine the components involved in this function of the Rim pathway, and whether it affects the accumulation of transporters in addition to Ena1 and if it is required for the full alkaline pH response.

Acknowledgements:

We thank Drs. J. M. Mulet, M. Proft, A. Mitchell and H. Sychrová for providing strains and plasmids and E. Sayas for technical assistance. This work was supported by grant BFU2011-30197-C03-03 from the Spanish Ministry of Science and Innovation (Madrid, Spain) and EUI2009-04147 [Systems Biology of Microorganisms (SysMo2) European Research Area-Network (ERA-NET)]. V. L-T. was supported by a pre-doctoral fellowship from the Polytechnic University of Valencia.

References:

Abriel H, Loffing J, Rebhun JF, Pratt JH, Schild L, Horisberger JD, Rotin D & Staub O (1999) Defective regulation of the epithelial Na+ channel by Nedd4 in Liddle's syndrome. *J Clin Invest* **103**: 667-673.

Alepuz PM, Cunningham KW & Estruch F (1997) Glucose repression affects ion homeostasis in yeast through the regulation of the stress-activated ENA1 gene. *Molecular Microbiology* **26**: 91-98.

Arino J, Ramos J & Sychrova H (2010) Alkali Metal Cation Transport and Homeostasis in Yeasts. *Microbiology and Molecular Biology Reviews* **74**: 95-+.

Bagnat M, Chang A & Simons K (2001) Plasma membrane proton ATPase Pma1p requires raft association for surface delivery in yeast. *Molecular Biology of the Cell* **12**: 4129-4138.

Bañuelos MA, Sychrová H, Bleykasten-Grosshans C, Souciet JL & Potier S (1998) The Nha1 antiporter of Saccharomyces cerevisiae mediates sodium and potassium efflux. *Microbiology* **144 (Pt 10)**: 2749-2758.

Boysen JH & Mitchell AP (2006) Control of Bro1-domain protein Rim20 localization by external pH, ESCRT machinery, and the Saccharomyces cerevisiae Rim101 pathway. *Molecular Biology of the Cell* **17**: 1344-1353.

Calcagno-Pizarelli AM, Hervas-Aguilar A, Galindo A, Abenza JF, Penalva MA & Arst HN, Jr. (2011) Rescue of Aspergillus nidulans severely debilitating null mutations in ESCRT-0, I, II and III genes by inactivation of a salt-tolerance pathway allows examination of ESCRT gene roles in pH signalling. *Journal of Cell Science* **124**: 4064-4076.

Chang SS, Grunder S, Hanukoglu A*, et al.* (1996) Mutations in subunits of the epithelial sodium channel cause salt wasting with hyperkalaemic acidosis, pseudohypoaldosteronism type 1. *Nature Genetics* **12**: 248-253.

Crespo JL, Daicho K, Ushimaru T & Hall MN (2001) The GATA transcription factors GLN3 and GAT1 link TOR to salt stress in Saccharomyces cerevisiae. *Journal of Biological Chemistry* **276**: 34441-34444.

Galindo A, Calcagno-Pizarelli AM, Arst HN & Peñalva M (2012) An ordered pathway for the assembly of fungal ESCRT-containing ambient pH signalling complexes at the plasma membrane. *J Cell Sci* **125**: 1784-1795.

Garí E, Piedrafita L, Aldea M & Herrero E (1997) A set of vectors with a tetracycline-regulatable promoter system for modulated gene expression in Saccharomyces cerevisiae. *Yeast* **13**: 837-848.

Gaxiola R, de Larrinoa IF, Villalba JM & Serrano R (1992) A novel and conserved salt-induced protein is an important determinant of salt tolerance in yeast. *EMBO J* **11**: 3157-3164.

Giaever G, Chu AM, Ni L*, et al.* (2002) Functional profiling of the Saccharomyces cerevisiae genome. *Nature* **418**: 387-391.

Hayashi M, Fukuzawa T, Sorimachi H & Maeda T (2005) Constitutive activation of the pH-responsive Rim101 pathway in yeast mutants defective in late steps of the MVB/ESCRT pathway. *Molecular and Cellular Biology* **25**: 9478-9490.

Herrador A, Herranz S, Lara D & Vincent O (2010) Recruitment of the ESCRT Machinery to a Putative Seven-Transmembrane-Domain Receptor Is Mediated by an Arrestin-Related Protein. *Molecular and Cellular Biology* **30**: 897-907.

Herranz S, Rodríguez JM, Bussink HJ, Sánchez-Ferrero JC, Arst HN, Peñalva MA & Vincent O (2005) Arrestin-related proteins mediate pH signaling in fungi. *Proc Natl Acad Sci U S A* **102**: 12141-12146.

Horak J (2003) The role of ubiquitin in down-regulation and intracellular sorting of membrane proteins: insights from yeast. *Biochimica Et Biophysica Acta-Biomembranes* **1614**: 139-155.

Ito T, Chiba T, Ozawa R, Yoshida M, Hattori M & Sakaki Y (2001) A comprehensive two-hybrid analysis to explore the yeast protein interactome. *Proc Natl Acad Sci U S A* **98**: 4569-4574.

Lamb TM & Mitchell AP (2003) The transcription factor Rim101p governs ion tolerance and cell differentiation by direct repression of the regulatory genes NRG1 and SMP1 in Saccharomyces cerevisiae. *Molecular and Cellular Biology* **23**: 677-686.

Lamb TM, Xu WJ, Diamond A & Mitchell AP (2001) Alkaline response genes of Saccharomyces cerevisiae and their relationship to the RIM101 pathway. *Journal of Biological Chemistry* **276**: 1850-1856.

Lauwers E, Erpapazoglou Z, Haguenauer-Tsapis R & Andre B (2010) The ubiquitin code of yeast permease trafficking. *Trends in Cell Biology* **20**: 196-204.

Leon S & Haguenauer-Tsapis R (2009) Ubiquitin ligase adaptors: Regulators of ubiquitylation and endocytosis of plasma membrane proteins. *Experimental Cell Research* **315**: 1574-1583.

Liu Y & Chang A (2006) Quality control of a mutant plasma membrane ATPase: ubiquitylation prevents cell-surface stability. *Journal of Cell Science* **119**: 360-369.

Logg K, Warringer J, Hashemi SH, Kall M & Blomberg A (2008) The sodium pump Ena1p provides mechanistic insight into the salt sensitivity of vacuolar protein sorting mutants. *Biochimica Et Biophysica Acta-Molecular Cell Research* **1783**: 974-984.

Longtine MS, McKenzie A, Demarini DJ, Shah NG, Wach A, Brachat A, Philippsen P & Pringle JR (1998) Additional modules for versatile and economical PCR-based gene deletion and modification in Saccharomyces cerevisiae. *Yeast* **14**: 953-961.

MacGurn JA, Hsu P-C & Emr SD (2012) Ubiquitin and Membrane Protein Turnover: From Cradle to Grave. *Annual Review of Biochemistry, Vol 81* **81**: 231-259.

Maeda T (2012) The signaling mechanism of ambient pH sensing and adaptation in yeast and fungi. *Febs Journal* **279**: 1407-1413.

Marquez JA & Serrano R (1996) Multiple transduction pathways regulate the sodium-extrusion gene PMR2/ENA1 during salt stress in yeast. *Febs Letters* **382**: 89-92.

Mulet JM, Llopis-Torregrosa V, Primo C, Marqués MC & Yenush L (2013) Endocytic regulation of alkali metal transport proteins in mammals, yeast and plants. *Curr Genet* **59**: 207-230.

Mulet JM, Leube MP, Kron SJ, Rios G, Fink GR & Serrano R (1999) A novel mechanism of ion homeostasis and salt tolerance in yeast: the Hal4 and Hal5 protein kinases modulate the Trk1-Trk2 potassium transporter. *Mol Cell Biol* **19**: 3328-3337.

Obara K & Kihara A (2014) Signaling events of the Rim101 pathway occur at the plasma membrane in a ubiquitination-dependent manner. *Mol Cell Biol* **34**: 3525-3534.

Perez-Valle J, Jenkins H, Merchan S, Montiel V, Ramos J, Sharma S, Serrano R & Yenush L (2007) Key role for intracellular K+ and protein kinases Sat4/Hal4 and Ha15 in the plasma membrane stabilization of yeast nutrient transporters. *Molecular and Cellular Biology* **27**: 5725-5736.

Perez-Valle J, Rothe J, Primo C, Martinez Pastor M, Arino J, Pascual-Ahuir A, Miguel Mulet J, Serrano R & Yenush L (2010) Hal4 and Hal5 Protein Kinases Are Required for General Control of Carbon and Nitrogen Uptake and Metabolism. *Eukaryotic Cell* **9**: 1881-1890.

Platara M, Ruiz A, Serrano R, Palomino A, Moreno F & Arino J (2006) The transcriptional response of the yeast Na+-ATPase ENA1 gene to alkaline stress involves three main signaling pathways. *Journal of Biological Chemistry* **281**: 36632-36642.

Proft M & Serrano R (1999) Repressors and upstream repressing sequences of the stress-regulated ENA1 gene in Saccharomyces cerevisiae: bZIP protein Sko1p confers HOG-dependent osmotic regulation. *Molecular and Cellular Biology* **19**: 537-546.

Rienzo A, Pascual-Ahuir A & Proft M (2012) The use of a real-time luciferase assay to quantify gene expression dynamics in the living yeast cell. *Yeast* **29**: 219-231.

Rotin D & Staub O (2011) Role of the ubiquitin system in regulating ion transport. *Pflugers Archiv-European Journal of Physiology* **461**: 1-21.

Ruiz A & Arino J (2007) Function and regulation of the Saccharomyces cerevisiae ENA sodium ATPase system. *Eukaryotic Cell* **6**: 2175-2183.

Schild L, Lu Y, Gautschi I, Schneeberger E, Lifton RP & Rossier BC (1996) Identification of a PY motif in the epithelial Na channel subunits as a target sequence for mutations causing channel activation found in Liddle syndrome. *The EMBO Journal* **15**: 2381-2387.

Serrano R, Ruiz A, Bernal D, Chambers JR & Arino J (2002) The transcriptional response to alkaline pH in Saccharomyces cerevisiae: evidence for calcium-mediated signalling. *Molecular Microbiology* **46**: 1319-1333.

Staub O, Dho S, Henry P, Correa J, Ishikawa T, McGlade J & Rotin D (1996) WW domains of Nedd4 bind to the proline-rich PY motifs in the epithelial Na+ channel deleted in Liddle's syndrome. *EMBO J* **15**: 2371-2380.

Subramanian S, Woolford CA, Desai JV, Lanni F & Mitchell AP (2012) cis- and trans-acting localization determinants of pH response regulator Rim13 in Saccharomyces cerevisiae. *Eukaryot Cell* **11**: 1201-1209.

Treton B, Blanchin-Roland S, Lambert M, Lepingle A & Gaillardin C (2000) Ambient pH signalling in ascomycetous yeasts involves homologues of the Aspergillus nidulans genes palF and palH. *Molecular and General Genetics* **263**: 505-513.

Vidan S & Mitchell AP (1997) Stimulation of yeast meiotic gene expression by the glucose-repressible protein kinase Rim15p. *Mol Cell Biol* **17**: 2688-2697.

Wadskog I, Forsmark A, Rossi G, Konopka C, Oyen M, Goksör M, Ronne H, Brennwald P & Adler L (2006) The yeast tumor suppressor homologue Sro7p is required for targeting of the sodium pumping ATPase to the cell surface. *Mol Biol Cell* **17**: 4988-5003.

Wang GL, Yang J & Huibregtse JM (1999) Functional domains of the Rsp5 ubiquitin-protein ligase. *Molecular and Cellular Biology* **19**: 342-352.

Xu WJ & Mitchell AP (2001) Yeast PalA/AIP1/Alix homolog Rim20p associates with a PEST-like region and is required for its proteolytic cleavage. *Journal of Bacteriology* **183**: 6917-6923.

Xu WJ, Smith FJ, Subaran R & Mitchell AP (2004) Multivesicular body-ESCRT components function in pH response regulation in Saccharomyces cerevisiae and Candida albicans. *Molecular Biology of the Cell* **15**: 5528-5537.

Yang B & Kumar S (2010) Nedd4 and Nedd4-2: closely related ubiquitin-protein ligases with distinct physiological functions. *Cell Death and Differentiation* **17**: 68-77.

Yoshikawa K, Tanaka T, Furusawa C, Nagahisa K, Hirasawa T & Shimizu H (2009) Comprehensive phenotypic analysis for identification of genes affecting growth under ethanol stress in Saccharomyces cerevisiae. *Fems Yeast Research* **9**: 32-44.

Zahrádka J & Sychrová H (2012) Plasma-membrane hyperpolarization diminishes the cation efflux via Nha1 antiporter and Ena ATPase under potassium-limiting conditions. *FEMS Yeast Res* **12**: 439-446.

Zhao J, Lin W, Ma X, Lu Q, Ma X, Bian G & Jiang L (2010) The protein kinase Hal5p is the high-copy suppressor of lithium-sensitive mutations of genes involved in the sporulation and meiosis as well as the ergosterol biosynthesis in Saccharomyces cerevisiae. *Genomics* **95**: 290-298.

Figure Legends:

Figure 1. Salt sensitivity of Rsp5 adapter mutants. The indicated strains were grown to saturation, serially diluted and spotted onto the indicated media. Images were taken after 2-5 days incubation. Similar results were observed in three independent experiments.

Figure 2. *ENA1* mRNA expression in *rim8* and *rim101* mutants. The induction of the *ENA1* mRNA in response to mild salt stress (0.5 M NaCl) was monitored by real-time luciferase assays (A) northern blot (B) and beta-galactosidase activity (C). (A) *ENA1* expression was monitored using the real-time luciferase assay (Rienzo *et al.*, 2012). Data are expressed as fold-induction setting the luciferase signal at time 0 to 1. Each point represents the average of 9 independent determinations (triplicate determinations in three independent experiments). The error bars indicate the standard deviation. (B) The *ENA1* mRNA signal was normalized using *TBP1* and the results are expressed as relative induction of *ENA1* (WT time 15 = 100%). Data represent the results of three separate experiments and the error bars represent the standard deviation. (C) Beta-galactosidase assays were performed using the full *ENA1* promoter. Data represent the average of three technical replicates obtained from two independent clones. The error bars indicate the standard deviation.

Figure 3. Ena1 protein levels and Na^+ loading and extrusion in *rim8* and *rim101* mutants. (A) Ena1 protein levels were monitored by anti-GFP immunoblots of protein recovered from the indicated strains treated with 0.5 M NaCl harbouring a genomic integration of the GFP coding sequence at the *ENA1* C-terminus. Note that whereas the blots of the WT and *crz1* mutants were exposed for 3 minutes, the blots corresponding to *rim8* and *rim101* were exposed for 20 minutes to detect the very low Ena1 signal. Molecular weight markers are shown on the left and the bottom panel shows the Direct Blue staining of the membrane as a loading control. Similar results were observed in three independent experiments. (B) The indicated strains were grown to exponential phase and then transferred to media containing 0.5 M NaCl. The amount of intracellular Na^+ at each time point was determined as described in Experimental Procedures. (C) The same cultures were then washed and resuspended in media with no NaCl. Samples were taken at the indicated times and the amount of intracellular Na^+ was determined. Data are expressed as a percentage of the Na^+ content at time 0. In both experiments, data are the average of three replicates and the error bars represent the standard deviation. Similar results were obtained in two separate experiments. (*= p value < 0.025; ** = p value < 0.005)

Figure 4. Phenotypic rescue of the *rim8* mutant by the constitutively active *RIM101-511* allele. (A) The indicated strains were grown to saturation, serially diluted and spotted onto the indicated media. Images were taken after 2-5 days incubation. Similar results were observed in three independent clones. (B) Ena1 protein levels were

monitored by anti-GFP immunoblots of protein recovered from the indicated strains harbouring a genomic integration of the GFP coding sequence at the *ENA1* C-terminus transformed with the empty plasmid or the *RIM101-511* allele and treated or not with 0.5 M NaCl for 60 minutes. Molecular weight markers are shown on the left and the bottom panel shows the Direct Blue staining of the membrane as a loading control. Similar results were observed in three independent experiments.

Figure 5. Analysis of the phenotype, protein profile and localization of YEp-*ENA1-GFP* in *rim8* and *rim101* mutants. (A) The indicated strains were grown to saturation, serially diluted and spotted onto the indicated media. Images were taken after 2-5 days incubation. Similar results were observed in three independent clones. (B) Cultures were grown to mid-log phase and the cell were washed and resuspended in the absence of doxycycline to induce *ENA1*-GFP expression (IND. = induction). Samples were harvested at the indicated times, the extracted proteins were processed as described in Experimental Procedures and analyzed by immunoblotting with anti-GFP. (1 = WT; 2 = *rim8*; 3 = *rim101*). Molecular weight markers are shown on the left and the bottom panel shows the Direct Blue staining of the membrane as a loading control. Similar results were observed in two different clones. (C) The localization of Ena1-GFP was analyzed by confocal microscopy. Cells were treated as described above. Images of representative cells are shown for each genotype.

Figure 6. Analysis of Tat2 levels and Mup1 delivery in *rim8* and *rim101* mutants. Wild type (1), *rim8* (2) and *rim101* (3) strains were transformed with a *TAT2*-GFP or *MUP1*-GFP containing plasmid. (A) Cells were grown to exponential phase and the amount of Tat2-GFP was determined. (B) Cells were grown to exponential phase in methionine-containing media, washed and then resuspended in media without methionine (- Met). Samples were taken at the indicated times and the amount of Mup1-GFP was determined. In both cases, the amount of permease was determined by immunodetection of transferred proteins with anti-GFP antibodies. The molecular weight markers are indicated on the left and the scanned image of the Direct Blue-stained membrane is shown in the bottom panel as a loading control. Similar results were observed in two different experiments.

Figure 7. Salt sensitivity and Ena1-GFP protein profile in Rim101 pathway mutants. (A) The growth phenotypes of the indicated strains were determined as described in Figure 1. Identical results were observed for three different clones. (B) The Ena1-GFP protein profile was determined in the indicated strains as described in Figure 4B (Induction time = 4 hours). Similar results were observed in three independent experiments.

Figure 8. Salt sensitivity and Ena1-GFP protein profile in ESCRT mutants. (A) The growth phenotypes of the indicated strains were determined as described in Figure 1. Identical results were observed for three different clones. (B) The Ena1-GFP protein

profile was determined in the indicated strains as described in Figure 4B (Induction time = 4 hours). Similar results were observed in three independent experiments.

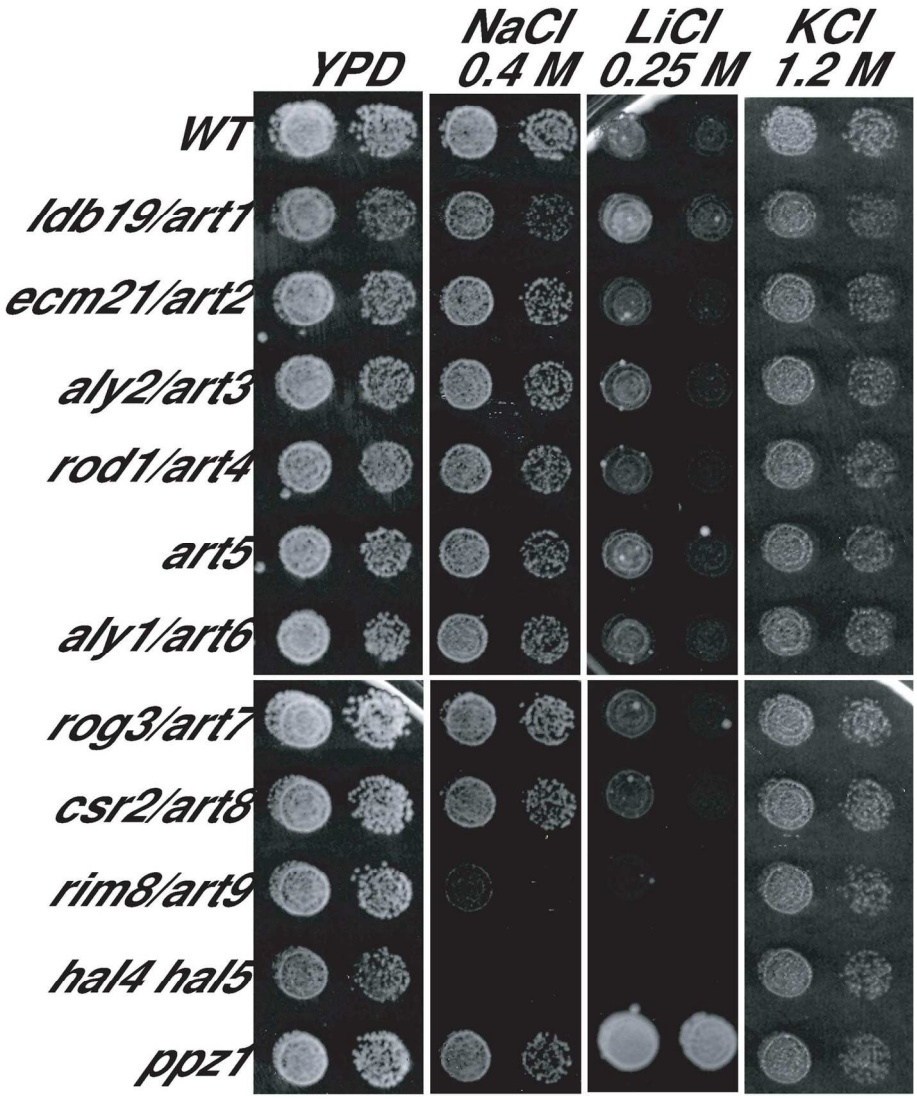

Fig. 1

Figure 1. Salt sensitivity of Rsp5 adapter mutants. The indicated strains were grown to saturation, serially diluted and spotted onto the indicated media. Images were taken after 2-5 days incubation. Similar results were observed in three independent experiments.
128x168mm (300 x 300 DPI)

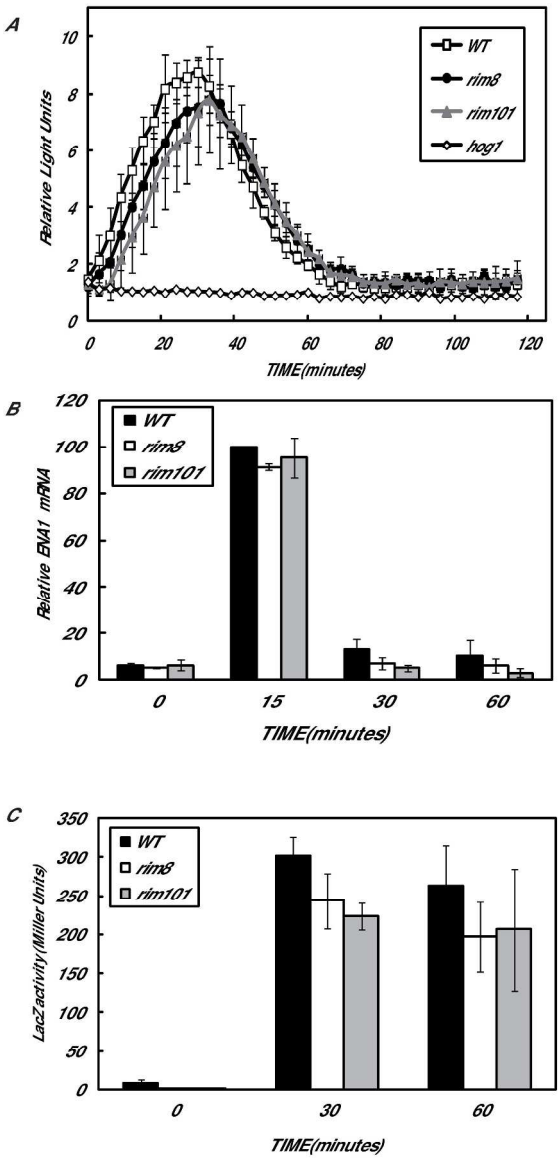

Fig. 2

Figure 2. ENA1 mRNA expression in rim8 and rim101 mutants. The induction of the ENA1 mRNA in response to mild salt stress (0.5 M NaCl) was monitored by real-time luciferase assays (A) northern blot (B) and beta-galactosidase activity (C). (A) ENA1 expression was monitored using the real-time luciferase assay (Rienzo et al., 2012). Data are expressed as fold-induction setting the luciferase signal at time 0 to 1. Each point represents the average of 9 independent determinations (triplicate determinations in three independent experiments). The error bars indicate the standard deviation. (B) The ENA1 mRNA signal was normalized using TBP1 and the results are expressed as relative induction of ENA1 (WT time 15 = 100%). Data represent the results of three separate experiments and the error bars represent the standard deviation. (C) Beta-galactosidase assays were performed using the full ENA1 promoter. Data represent the average of three technical replicates obtained from two independent clones. The error bars indicate the standard deviation.
272x487mm (300 x 300 DPI)

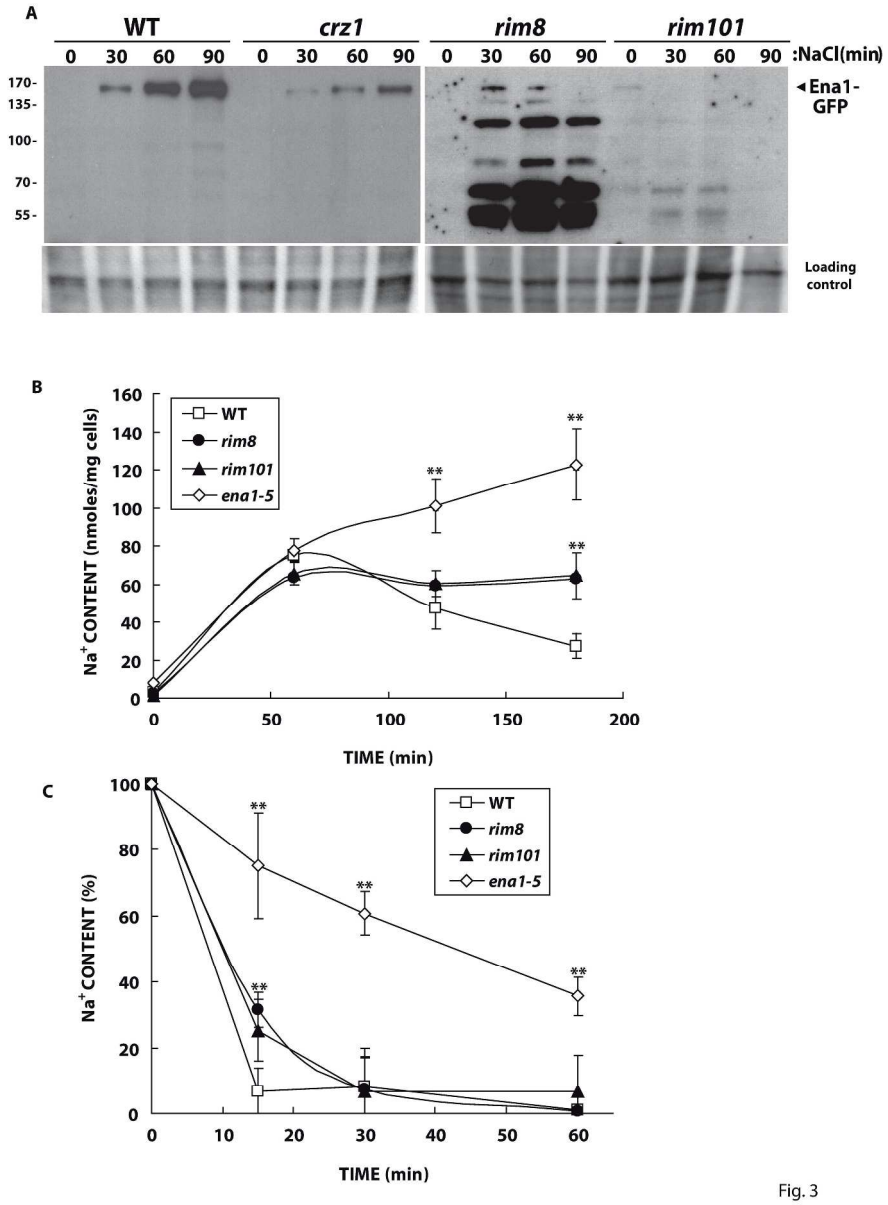

Fig. 3

Figure 3. Ena1 protein levels and Na+ loading and extrusion in rim8 and rim101 mutants. (A) Ena1 protein levels were monitored by anti-GFP immunoblots of protein recovered from the indicated strains treated with 0.5 M NaCl harbouring a genomic integration of the GFP coding sequence at the ENA1 C-terminus. Note that whereas the blots of the WT and crz1 mutants were exposed for 3 minutes, the blots corresponding to rim8 and rim101 were exposed for 20 minutes to detect the very low Ena1 signal. Molecular weight markers are shown on the left and the bottom panel shows the Direct Blue staining of the membrane as a loading control. Similar results were observed in three independent experiments. (B) The indicated strains were grown to exponential phase and then transferred to media containing 0.5 M NaCl. The amount of intracellular Na+ at each time point was determined as described in Experimental Procedures. (C) The same cultures were then washed and resuspended in media with no NaCl. Samples were taken at the indicated times and the amount of intracellular Na+ was determined. Data are expressed as a percentage of the Na+ content at time 0. In both experiments, data are the average of three replicates and the error bars represent the standard deviation. Similar results were obtained in two separate experiments. (*= p value <

0.025; ** = p value < 0.005)
271x372mm (300 x 300 DPI)

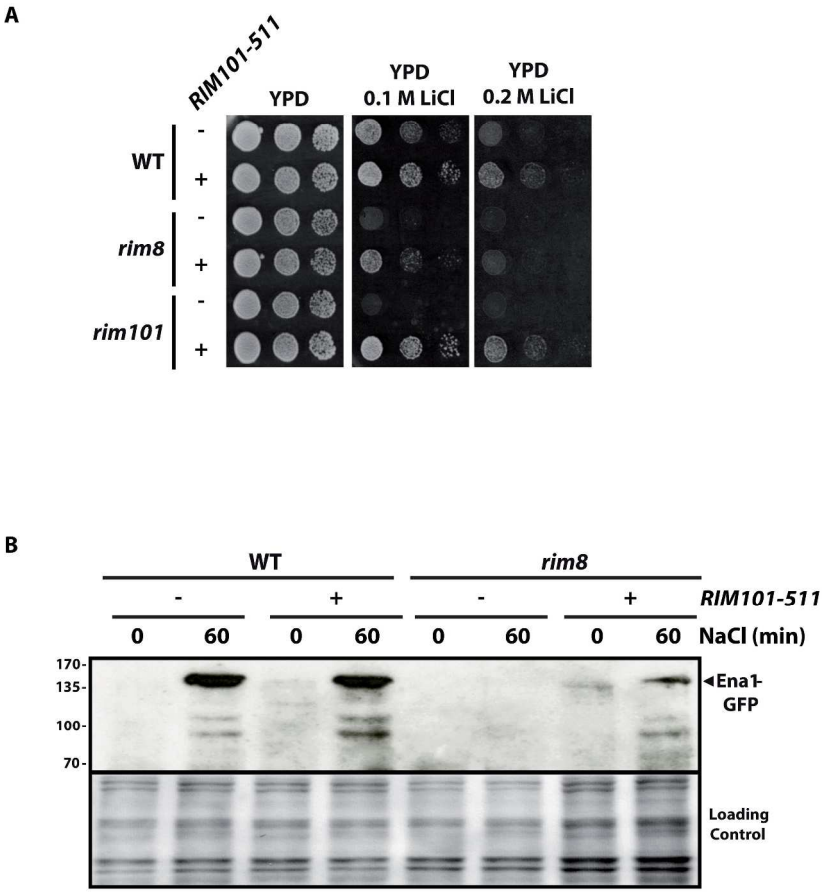

Fig 4

Figure 4. Phenotypic rescue of the rim8 mutant by the constitutively active RIM101-511 allele. (A) The indicated strains were grown to saturation, serially diluted and spotted onto the indicated media. Images were taken after 2-5 days incubation. Similar results were observed in three independent clones. (B) Ena1 protein levels were monitored by anti-GFP immunoblots of protein recovered from the indicated strains harbouring a genomic integration of the GFP coding sequence at the ENA1 C-terminus transformed with the empty plasmid or the RIM101-511 allele and treated or not with 0.5 M NaCl for 60 minutes. Molecular weight markers are shown on the left and the bottom panel shows the Direct Blue staining of the membrane as a loading control. Similar results were observed in three independent experiments.
255x375mm (300 x 300 DPI)

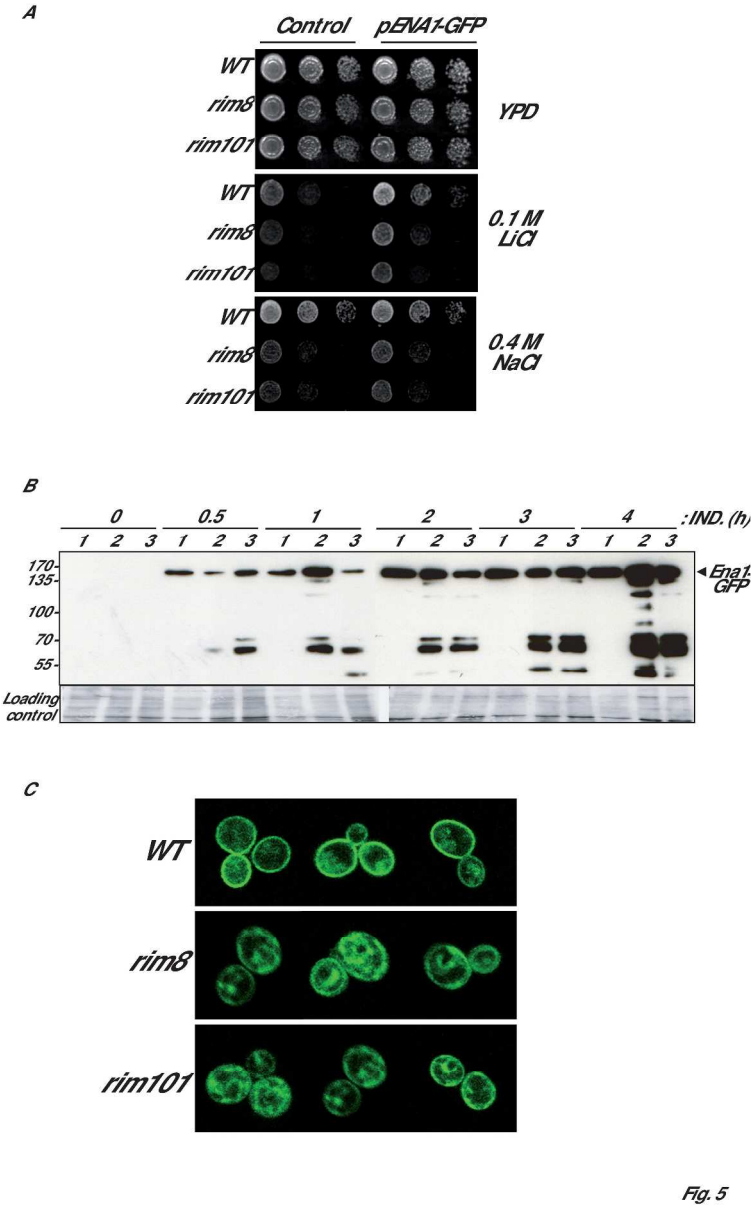

Figure 5. Analysis of the phenotype, protein profile and localization of YEp-ENA1-GFP in rim8 and rim101 mutants. (A) The indicated strains were grown to saturation, serially diluted and spotted onto the indicated media. Images were taken after 2-5 days incubation. Similar results were observed in three independent clones. (B) Cultures were grown to mid-log phase and the cell were washed and resuspended in the absence of doxycycline to induce ENA1-GFP expression (IND. = induction). Samples were harvested at the indicated times, the extracted proteins were processed as described in Experimental Procedures and analyzed by immunoblotting with anti-GFP. (1 = WT; 2 = rim8; 3 = rim101). Molecular weight markers are shown on the left and the bottom panel shows the Direct Blue staining of the membrane as a loading control. Similar results were observed in two different clones. (C) The localization of Ena1-GFP was analyzed by confocal microscopy. Cells were treated as described above. Images of representative cells are shown for each genotype.
277x445mm (300 x 300 DPI)

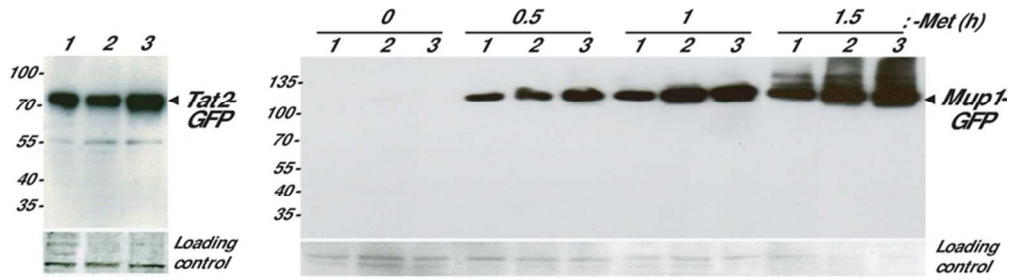

Fig. 6

Figure 6. Analysis of Tat2 levels and Mup1 delivery in rim8 and rim101 mutants. Wild type (1), rim8 (2) and rim101 (3) strains were transformed with a TAT2-GFP or MUP1-GFP containing plasmid. (A) Cells were grown to exponential phase and the amount of Tat2-GFP was determined. (B) Cells were grown to exponential phase in methionine-containing media, washed and then resuspended in media without methionine (- Met). Samples were taken at the indicated times and the amount of Mup1-GFP was determined. In both cases, the amount of permease was determined by immunodetection of transferred proteins with anti-GFP antibodies. The molecular weight markers are indicated on the left and the scanned image of the Direct Blue-stained membrane is shown in the bottom panel as a loading control. Similar results were observed in two different experiments.
71x26mm (300 x 300 DPI)

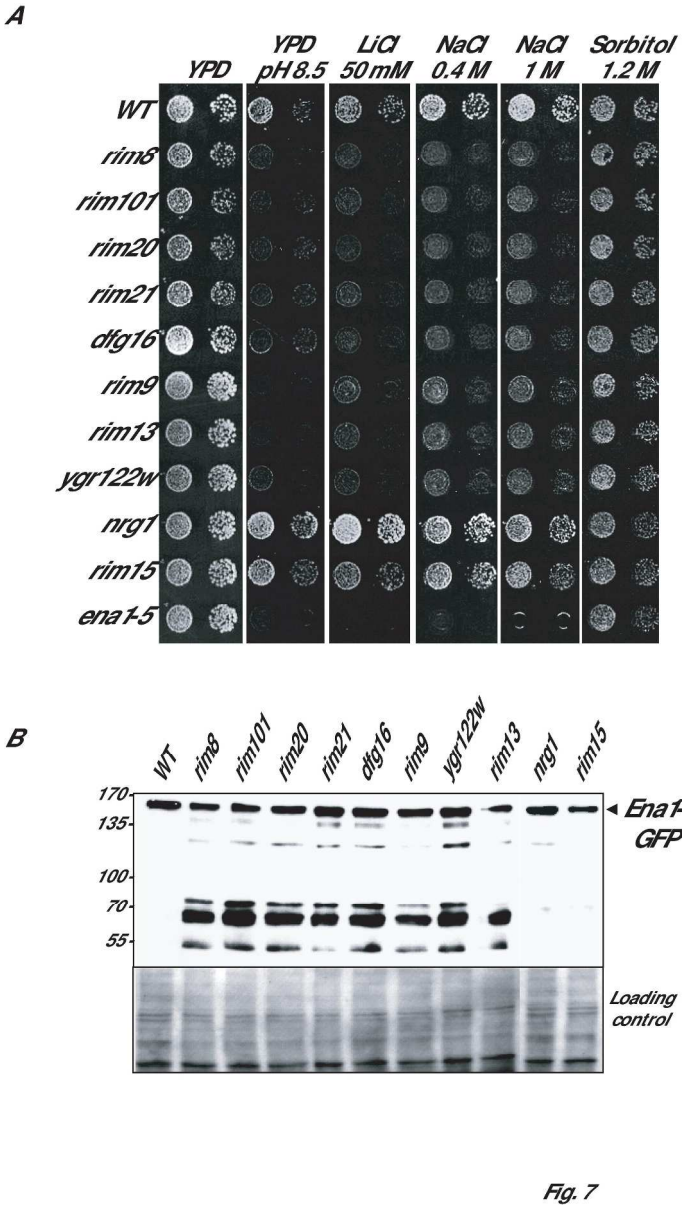

Fig. 7

Figure 7. Salt sensitivity and Ena1-GFP protein profile in Rim101 pathway mutants. (A) The growth phenotypes of the indicated strains were determined as described in Figure 1. Identical results were observed for three different clones. (B) The Ena1-GFP protein profile was determined in the indicated strains as described in Figure 4B (Induction time = 4 hours). Similar results were observed in three independent experiments.
236x418mm (300 x 300 DPI)

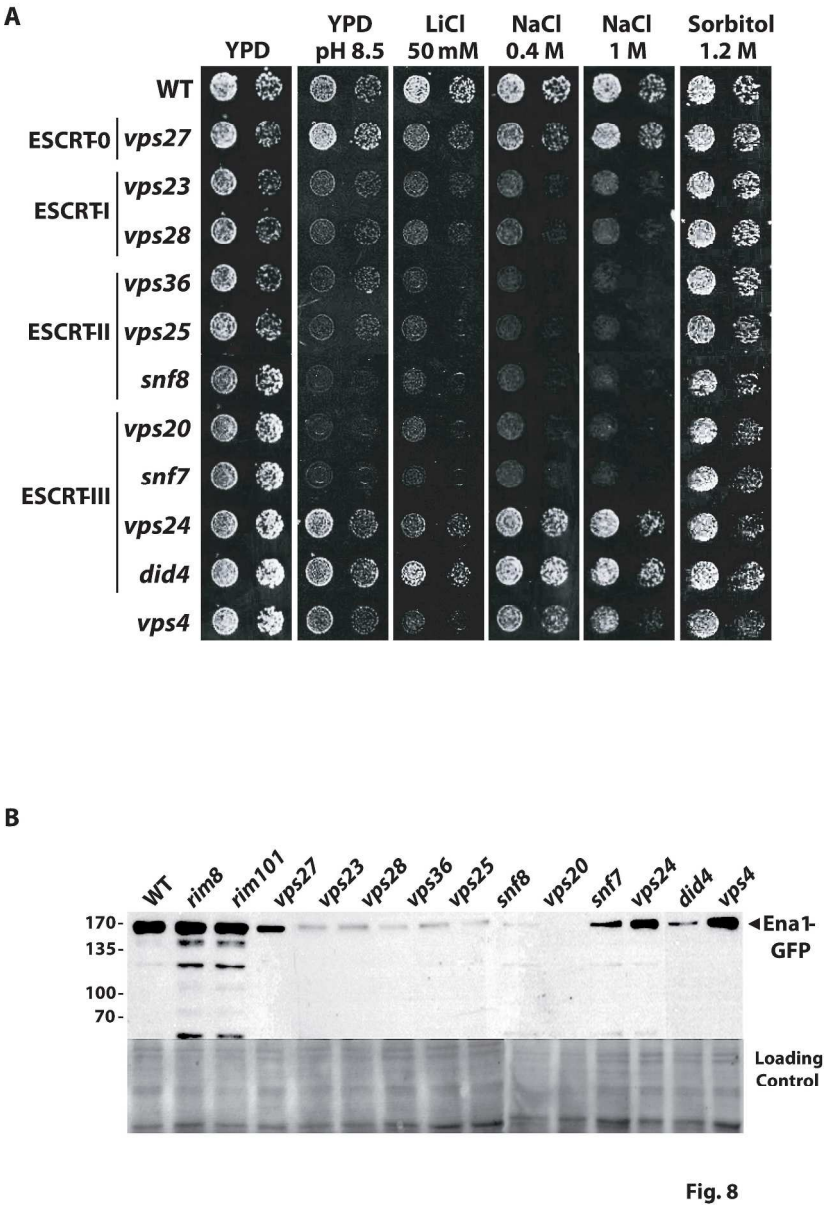

Figure 8. Salt sensitivity and Ena1-GFP protein profile in ESCRT mutants. (A) The growth phenotypes of the indicated strains were determined as described in Figure 1. Identical results were observed for three different clones. (B) The Ena1-GFP protein profile was determined in the indicated strains as described in Figure 4B (Induction time = 4 hours). Similar results were observed in three independent experiments.
227x334mm (300 x 300 DPI)